

WL-TR-91-4008

AD-A232 550

**POST-OVERLOAD FATIGUE CRACK RECOVERY
IN POWDER METAL ALUMINUM-LITHIUM AL-905XL
FORGING**



Russell R. Cervay
University of Dayton Research Institute
300 College Park Avenue
Dayton, Ohio 45469-0136

JANUARY 1991

Interim Report for the Period August 1989 - September 1990

Approved for Public Release; Distribution Unlimited.

DTIC
ELECTE
MAR 11 1991
S B D

**MATERIALS LABORATORY
WRIGHT RESEARCH AND DEVELOPMENT CENTER
AIR FORCE SYSTEMS COMMAND
WRIGHT-PATTERSON AIR FORCE BASE, OHIO 45433-6533**

91 3 05 063

NOTICE

When Government drawings, specifications, or other data are used for any purpose other than in connection with a definitely Government-related procurement, the United States Government incurs no responsibility or any obligation whatsoever. The fact that the Government may have formulated or in any way supplied the said drawings, specifications, or other data, is not to be regarded by implication, or otherwise in any manner construed, as licensing the holder, or any other person or corporation; or as conveying any rights or permission to manufacture, use, or sell any patented invention that may in any way be related thereto.

This report has been reviewed by the Office of Public Affairs (ASD/PA) and is releasable to the National Technical Information Service (NTIS). At NTIS is will be available to the general public including foreign nations.

This technical report has been reviewed and is approved for publication.

Mary Ann Phillips
MS. MARY ANN PHILLIPS
Engineering and Design Data
Materials Engineering Branch

Clayton L. Harmsworth
CLAYTON L. HARMSWORTH
Technical Manager
Engineering and Design Data
Materials Engineering Branch

FOR THE COMMANDER

T. J. Reinhardt
T. J. REINHART, Chief
Materials Engineering Branch
Materials Laboratory

If your address has changed, if you wish to be removed from our mailing list, or if the addressee is no longer employed by your organization, please notify WRDC/MLSE, Wright-Patterson AFB, OH 45433-6533 to help maintain a current mailing list.

Copies of this report should not be returned unless return is required by security considerations, contractual obligations, or notice on a specific document.

UNCLASSIFIED

SECURITY CLASSIFICATION OF THIS PAGE

REPORT DOCUMENTATION PAGE				Form Approved OMB No. 0704-0188
1a REPORT SECURITY CLASSIFICATION Unclassified		1b RESTRICTIVE MARKINGS		
2a SECURITY CLASSIFICATION AUTHORITY		3 DISTRIBUTION/AVAILABILITY OF REPORT Approved for Public Release; distribution unlimited.		
2b DECLASSIFICATION/DOWNGRADING SCHEDULE				
4 PERFORMING ORGANIZATION REPORT NUMBER(S) UDR-TR-90-102		5. MONITORING ORGANIZATION REPORT NUMBER(S) WL-TR-91-4008		
6a NAME OF PERFORMING ORGANIZATION University of Dayton Research Institute	6b. OFFICE SYMBOL (If applicable)	7a. NAME OF MONITORING ORGANIZATION Materials Laboratory (WRDC/MLSE) Wright Research and Development Center		
6c. ADDRESS (City, State, and ZIP Code) 300 College Park Avenue Dayton, OH 45469-0138	7b. ADDRESS (City, State, and ZIP Code) Wright-Patterson AFB, OH 45433-6533			
8a. NAME OF FUNDING/SPONSORING ORGANIZATION	8b. OFFICE SYMBOL (If applicable)	9 PROCUREMENT INSTRUMENT IDENTIFICATION NUMBER F33615-88-C-5437		
8c. ADDRESS (City, State, and ZIP Code)		10. SOURCE OF FUNDING NUMBERS		
		PROGRAM ELEMENT NO.	PROJECT NO.	TASK NO.
		62102F	2418	07
				03
11. TITLE (Include Security Classification) Post-Overload Fatigue Crack Recovery in Powder Metal Aluminum-Lithium AL-905XL Forging				
12. PERSONAL AUTHOR(S) Russell R. Cervay				
13a. TYPE OF REPORT Interim	13b. TIME COVERED FROM 8/89 TO 9/90	14. DATE OF REPORT (Year, Month, Day) January 1991	15. PAGE COUNT 36	
16. SUPPLEMENTARY NOTATION				
17. COSATI CODES		18. SUBJECT TERMS (Continue on reverse if necessary and identify by block number)		
FIELD	GROUP	SUB-GROUP	Powder Metal Fatigue Crack Growth Overload Crack Closure Retardation A1 905XL Forging	
19 ABSTRACT (Continue on reverse if necessary and identify by block number)				
<p>An overload fatigue investigation was conducted to determine whether variation in the relative humidity would effect the post-overload retardation recovery period of a dispersion hardened powder metal aluminum, alloy AL905XL forging. Constant amplitude and single spike overload tests were conducted in laboratory air, and in low and high humidity air environments. Post-overload crack opening load and crack propagation velocity were observed to determine the number of delay cycles required for the velocity and crack opening load to return to the values immediately preceding overload. Crack retardation increased in the high humidity environment and for shorter crack lengths attributable to increased crack closure.</p>				
20 DISTRIBUTION/AVAILABILITY OF ABSTRACT <input checked="" type="checkbox"/> UNCLASSIFIED/UNLIMITED <input type="checkbox"/> SAME AS RPT <input type="checkbox"/> DTIC USERS		21. ABSTRACT SECURITY CLASSIFICATION Unclassified		
22a. NAME OF RESPONSIBLE INDIVIDUAL Mary Ann Phillips		22b. TELEPHONE (Include Area Code) (513) 255-5128	22c. OFFICE SYMBOL WRDC/MLSE	

PREFACE

This technical report represents work conducted by the Materials Branch (WRDC/MLSE) of the System Support Division, Materials Laboratory, Wright Research and Development Center, WPAFB, Ohio, and supported by the University of Dayton Research Institute, Dayton, Ohio under Contract F33615-88-C-5437, "Quick Reaction Evaluation of Materials." Mr. Neal Ontko serves as current contract monitor.

Test control software was developed in August and September 1989. Testing of aluminum alloy 2091 took place from October 1989 through January 1990. Test of alloy AL-905XL covered from July through September 1990.

The author would like to extend recognition to Messrs. John Eblin and Donald Wolesslage of the University of Dayton who exercised great care in conducting the tests. The author would like to extend special recognition to Dr. Kumar V. Jata, also of the University of Dayton, for his advice and technical assistance in what was a new and unfamiliar technical area to the author and for his review of this document.

This report was submitted by the author in November 1990.

Accession For	
NTIS GRA&I	<input checked="" type="checkbox"/>
DTIC TAB	<input type="checkbox"/>
Unannounced	<input type="checkbox"/>
Justification	
By _____	
Distribution/	
Availability Codes	
Avail and/or	
Dist	Special
A-1	

TABLE OF CONTENTS

<u>SECTION</u>		<u>PAGE</u>
1	INTRODUCTION	1
2	BACKGROUND	3
3	TEST MATERIAL	10
4	PROCEDURES	12
5	RESULTS AND DISCUSSION	15
6	CONCLUSIONS	26
	REFERENCES	27

LIST OF FIGURES

<u>FIGURE</u>		<u>PAGE</u>
1	Post-Overload Normalized Velocity and Crack Opening Load Following an 80 Percent Overload on an Alloy 2091-T851 Plate Center Cracked Panel	4
2	Dual Location Back Face Strain Instrumentation of a Compact-Type Specimen	6
3	Post-Overload Normalized Velocity and Crack Opening Load Following a 100-Percent Overload on an Alloy 2091-T851 Plate Compact-Type Specimen	7
4	Post-Overload Normalized Velocity and Crack Opening Load Following an 80-Percent Overload on an Alloy 2091-T851 Plate Compact-Type Specimen	8
5	Constant Amplitude Loading High and Low Humidity Fatigue Crack Growth Test Results for Alloy AL-905XL Forging	16
6	Post-Overload Normalized Velocity and Crack Opening Load Following a 150-Percent Overload on an Alloy AL-905XL Compact-Type Specimen	17
7	Post-Overload Normalized Velocity and Crack Opening Load Following a 150-Percent Overload of an Alloy AL-905XL Compact-Type Specimen in Low Humidity Air	20
8	Post-Overload Normalized Velocity and Crack Opening Load Following a 150-Percent Overload of an Alloy AL-905XL Compact-Type Specimens in Laboratory Air	21
9	Post-Overload Normalized Velocity and Crack Opening Load Following a 150-Percent Overload of an Alloy AL-905XL Compact-Type Specimen in High Humidity Air	22
10	Alloy AL-905XL Normalized Crack Opening Load and Effective Stress Intensity Range for a Remote Stress Intensity Range Equal to 6 KSI $\sqrt{\text{in.}}$	23
11	Post-Overload Delay Cycles for Alloy AL-905XL Following a 150-Percent Overload	24

LIST OF TABLES

<u>TABLE</u>		<u>PAGE</u>
1	Tensile Properties of AL-905XL	10
2	PM Aluminum AL-905XL Forging Stress Corrosion Test Results	11
3	Aluminum Alloy AL-905XL Forging 150-Percent Overload Fatigue Test Results	14
4	Aluminum Alloy AL-905XL Forging 150-Percent Overload Fatigue Test Results	19

SECTION 1

INTRODUCTION

In the aerospace industry, there is a continuous quest for improved performance. The demand for lighter aerospace structural materials with no compromise in load carrying ability has given rise to the development of the lower density and higher stiffness aluminum-lithium alloys.

Constant amplitude loading fatigue crack growth rate testing is a useful tool for screening engineering materials and for evaluating various physical and metallurgical mechanisms. However, constant amplitude loading does not simulate service conditions and provide an accurate assessment of a structure's service life. For more accurate life prediction, spectrum loading is preferred. One of the mechanisms present in spectrum loading fatigue is increased compressive residual stress induced crack closure following a positive high load excursion (1). It has long been known that crack closure can account for the acceleration or retardation observed in propagating fatigue cracks (2). Increased crack closure results directly in considerable crack retardation following a tension overload. Aluminum lithium alloys have been shown to have a higher level of fatigue crack closure under variable amplitude conditions attributable to surface roughness of the crack faces (3-6). In adopting aluminum-lithium alloys, the structure benefits from an extended fatigue service life in addition to the already mentioned reduced weight, at a cost increase which is generally reasonable for most aerospace applications.

Variable amplitude loading experienced in service must be simulated in the laboratory, along with variations in relative humidity which also influence the fatigue crack growth rate in many high strength aluminum alloys. Higher humidity has been shown to increase stress corrosion cracking and the fatigue crack growth rate in aluminum alloy 7075 under both variable (7) and constant amplitude fatigue loading conditions (8). The test material, a dispersion hardened powder metal (PM) aluminum AL-905XL forging, is purported to have outstanding corrosion resistance (9). More conventional precipitation hardened aluminum-lithium alloys, containing copper, in addition to demonstrating excellent stress corrosion cracking resistance also show improved fatigue crack growth resistance in a high humidity environment in the threshold and near threshold regions (10). Fatigue crack growth retardation increases with additional copper content.

Consequently, a fatigue investigation was initiated to determine whether this fine grained, dispersion hardened, PM product, alloy AL-905XL, would also show improved fatigue crack growth resistance as does a precipitation hardened Al-Li product in a moist environment even though the test alloy contains no Cu, a strongly influential element with respect to fatigue crack growth retardation in a precipitation hardened Al-Li alloy. Variable and constant load amplitude tests were conducted in both low and high humidity environments as well as in laboratory air.

SECTION 2 BACKGROUND

Preliminary variable amplitude loading, i.e. overload, (OL), testing was done on aluminum alloy 2091-T851 rolled plate. The test specimen was a center cracked panel, M(T), 4 inches wide. Specimens were machined from a half-inch plate reduced in thickness to a quarter inch. A through-the-thickness machined slot 0.4 inch wide served as a fatigue crack starter notch. This specimen configuration was selected due to the original intention of including compression as well as tension overload in the investigation. For the OL test procedure, after shedding the stress intensity range, ΔK , to 6 KSI \sqrt{in} , a single 80 or 100 percent OL beyond the maximum dynamic load, P_{max} , was applied. Subsequent to the single overload cycle the pre-overload dynamic loading conditions were resumed. Crack velocity, V_i , and crack opening loads, Pop_i , were monitored and recorded for every ten thousands of an inch of crack extension. Recovery was taken to be when the crack velocity surpassed the pre-overload velocity and remained so. The crack lengths were monitored with Fractomat Krack Gage® (11). Determining the crack opening load of a M(T) panel proved to be difficult. The first approach for measurement of Pop_i , employed a MTS Model 632.05 crack mouth opening displacement gage (12) mounted on one of the panel faces across the crack plane. This instrument has good sensitivity with ± 0.020 -inch extension being its full range of travel. However, no consistent change in Pop_i could be perceived following the OL.

Some of the panels were then modified to include a lengthened crack starter notch plus a round hole tapered to the through-the-thickness center line to provide a knife edge. A transducer similar to an ASTM E399 (13) double cantilever displacement gage was altered to have half round ends and a V-groove to match the rounded knife edge at the panel's center. This improved the resolution for a crack length to width ratio, $2a/W$, exceeding 0.4. However, the scatter from cycle to cycle in Pop_i was in the range of the change generated by the overload.

The final approach at instrumenting the panels had strain gages bonded on both edges across the crack plane to monitor the back-face-strain (BFS). The results for one test are presented in Figure 1. In the figure, the post-overload crack velocity, V_i , is normalized by dividing that immediately preceding overload, V_0 ; as is the crack

AI-Li POST-OVERLOAD RETARDATION

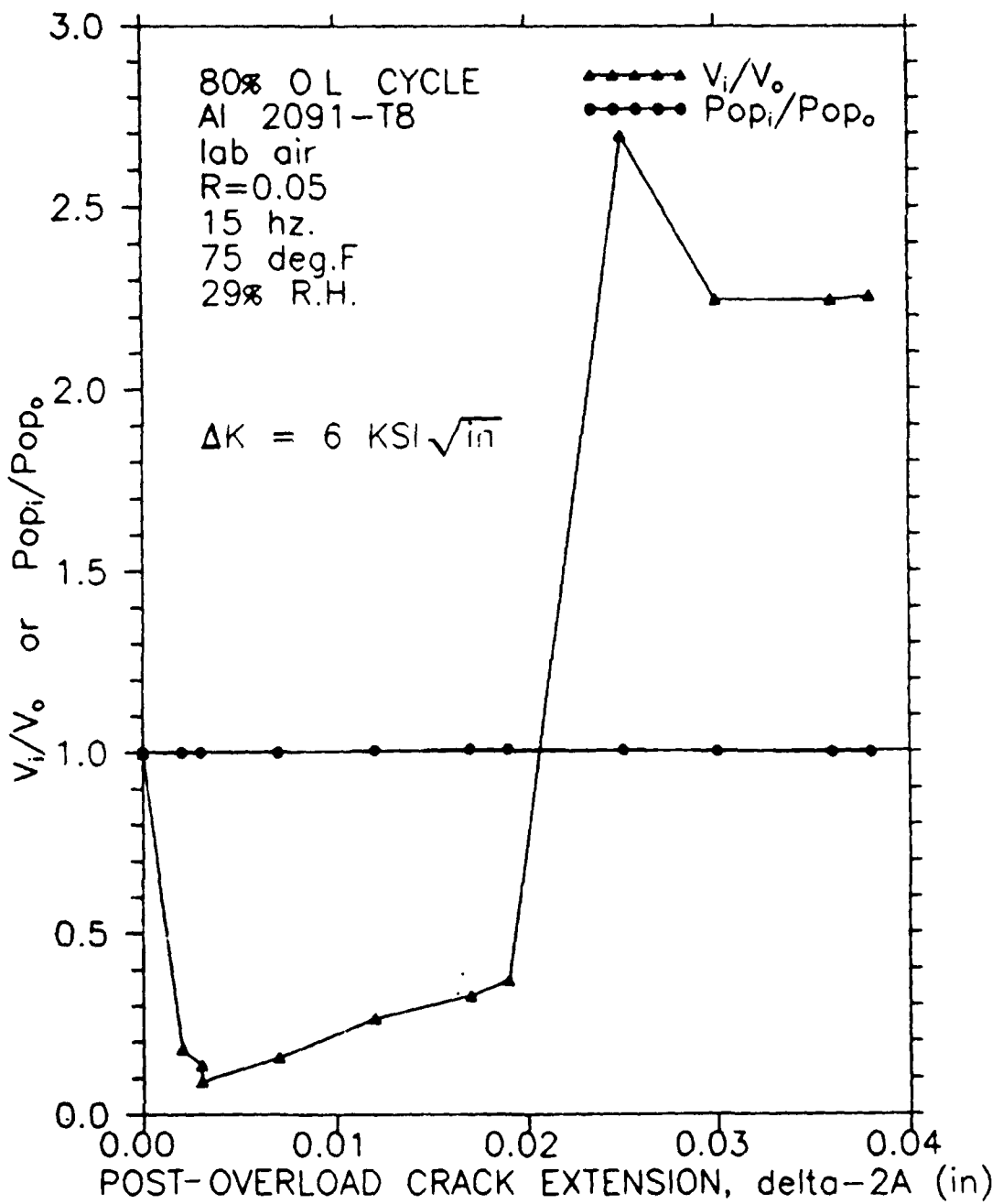


Figure 1. Post-Overload Normalized Velocity and Crack Opening Load Following an 80-Percent Overload on an Alloy 2091-T851 Plate Center Cracked Panel.

opening load, Pop_i normalized with that immediately prior to overload, Pop_0 . The line across the figure where V_i/V_0 and Pop_i/Pop_0 are equal to one henceforth will be referred to as the recovery line. This instrumentation improved the sensitivity and the cycle-to-cycle variation in Pop_0 was less than 1 percent for a/W greater than 0.4. The velocity trace crosses the recovery line following 280,000 cycles. For these tests, the changes in opening load, if any, was 2 percent or less. Still in more than half the tests, the 80-percent overload would dramatically reduce the velocity or even arrest the crack for hundreds of thousands of load cycles while the instrumentation could not detect any change in crack opening load. This was the same findings as K.T. Venkateswara Rao and R.O. Ritchie (6).

At this point the M(T) specimen was abandoned, and compression overloads were dropped from any further consideration. Some of the remaining test coupons were machined into compact type C(T) test specimens with an (L-T) orientation.

The dual location back-face strain compliance technique (14), illustrated in Figure 2 was used to measure the crack-opening-load. The dual location technique has been shown to provide more resolution with less amplification than the single location BFS technique (7) when the normalized crack length a/W is less than 0.4. The crack length was measured using Fractomat Krack Gage® as was done on the M(T) specimens. A number of refinements were made to the test control software such as recording data for every 0.005 inch of crack extension and an even smaller interval for the first 10 mils of post-overload crack growth.

The cycle-to-cycle scatter in Pop_i was reduced to be a fraction of a percent of P_{max} and test-to-test repeatability in laboratory air, with humidity below 30 percent, was considerably improved. The results for a 100-percent overload test are presented in Figure 3. The delay was 376 kilocycles, most of which the crack front was stationary, the crack opening load rose about 5 percent, and the velocity recovered following less than 10 mils of crack extension. In repeating the test, a 100-percent OL produced permanent crack arrest more often than not. The results for an 80-percent OL are plotted in Figure 4. As with A. Perkins (16) findings the 80-percent OL produced a considerable number of delay cycles but always allowed the velocity to recover. In this case the delay represents 345 kilocycles.

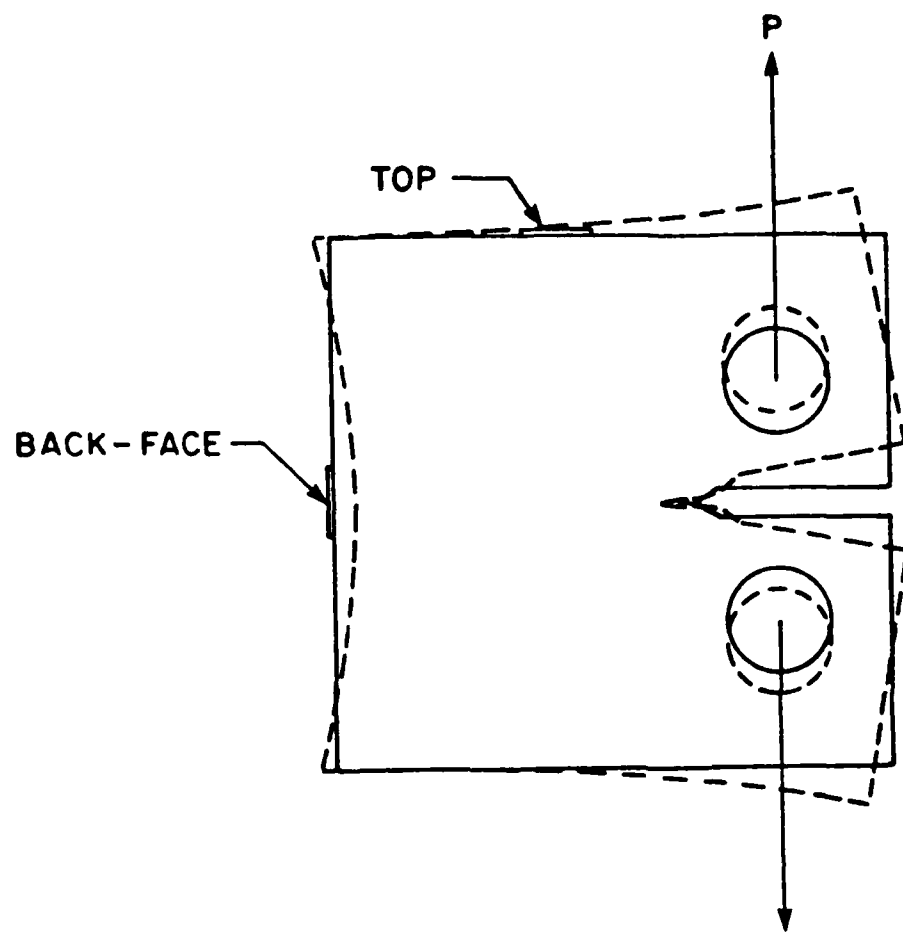


Figure 2. Dual Location Back Face Strain Instrumentation of a Compact-Type Specimen.

Al-Li POST-OVERLOAD RETARDATION

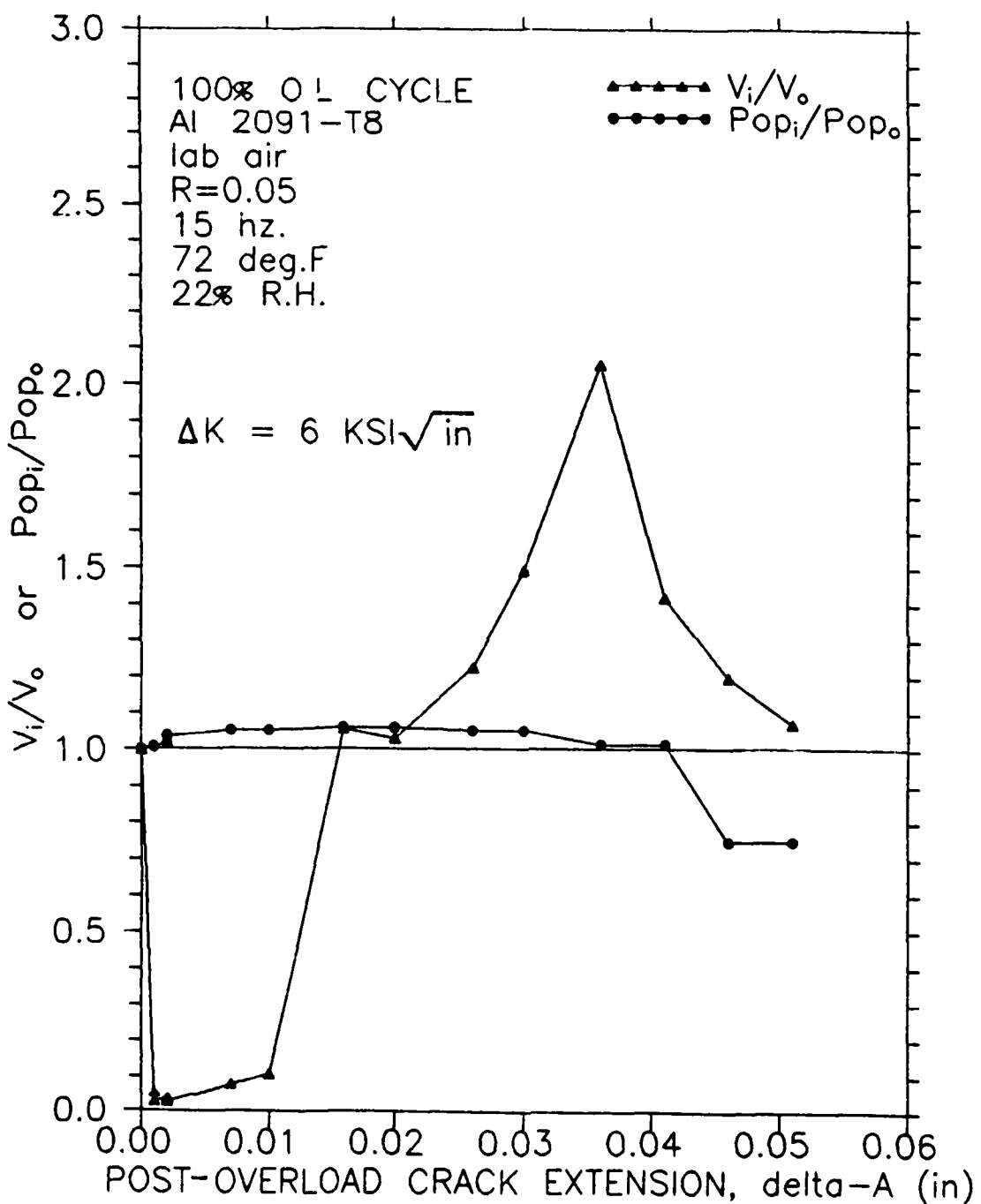


Figure 3. Post-Overload Normalized Velocity and Crack Opening Load Following a 100-Percent Overload on an Alloy 2091-T851 Plate Compact-Type Specimen.

AI-Li POST-OVERLOAD RETARDATION

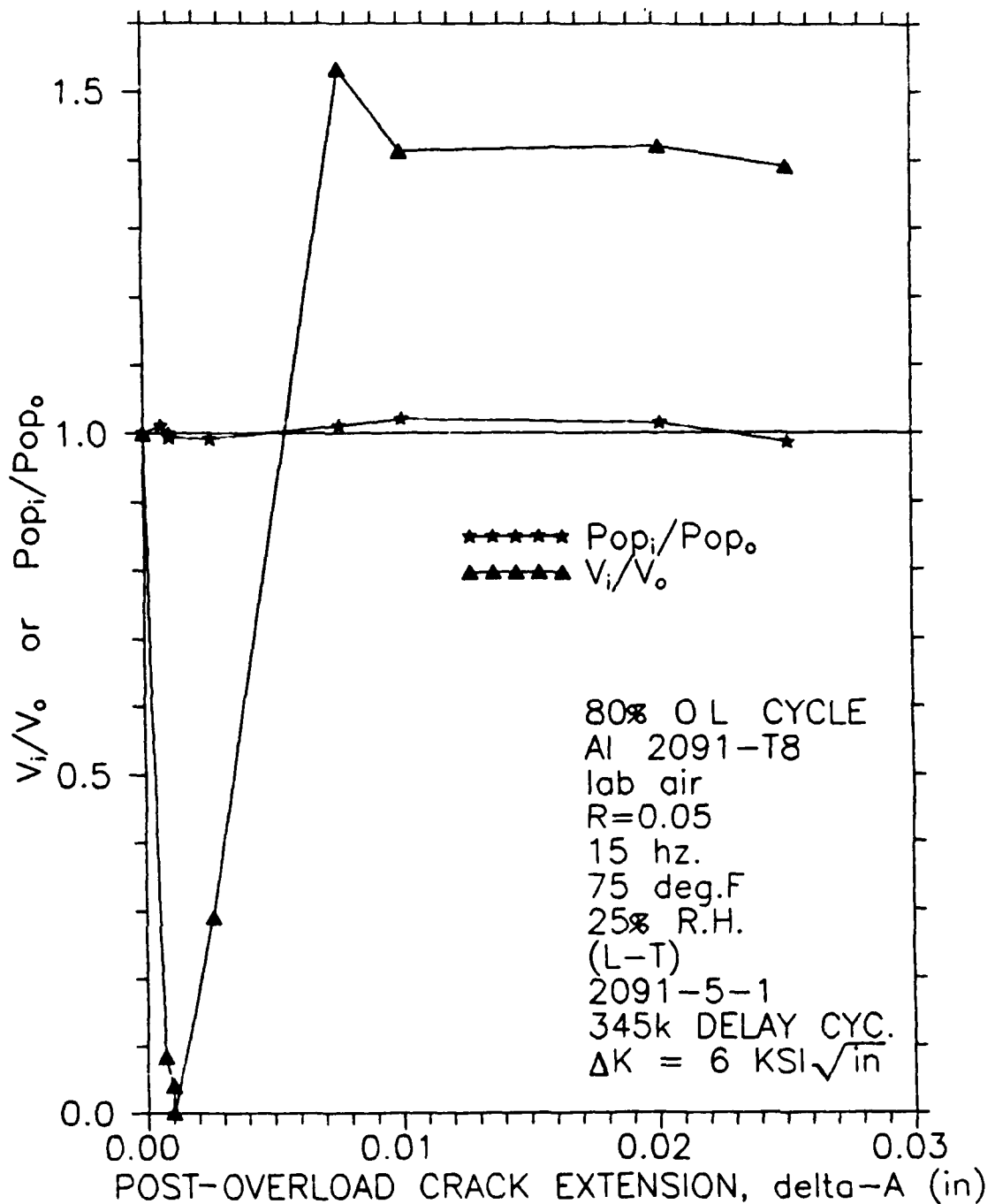


Figure 4. Post-Overload Normalized Velocity and Crack Opening Load Following an 80-Percent Overload on an Alloy 2091-T851 Plate Compact-Type Specimen.

With the test procedure, test control and data acquisition software, and instrumentation adequately refined attention was turned to material of primary interest PM aluminum alloy AL-905XL forging.

SECTION 3

TEST MATERIAL

The test material was mechanically alloyed PM aluminum alloy AL-905XL forging produced by Inco Alloys. The billets were hand forgings measured 1.25 x 6 x 9 inches and were produced in the fall of 1988. The results of a chemical constituent analysis are presented below:

CHEMICAL COMPOSITION, WEIGHT PERCENT

<u>Mg</u>	<u>C</u>	<u>Li</u>	<u>Si</u>	<u>Q</u>	<u>Al</u>
5.15	1.09	0.55	0.32	0.05	Balance

The material is under development for forging applications as a replacement to aluminum alloy 7075. It has been purported to possess good strength and ductility along with excellent resistance to stress corrosion. In addition, it is also claimed not to show anisotropic tensile properties as found in melted product forms (17).

All specimen blanks for this program were removed from the forging with the loading direction parallel to the longest billet dimensions. Tensile specimens were made and tested in accord with ASTM E8-89G (18). The results are presented below in Table 1.

TABLE 1
TENSILE PROPERTIES OF AL-905XL

<u>0.2% Yield Strength (ksi)</u>	<u>Ultimate Strength (ksi)</u>	<u>Reduction in Area (%)</u>	<u>Elongation (%)</u>
64.1	74.4	20.0	10.58
65.7	74.1	19.5	9.15
59.7	73.9	22.2	11.18

The test materials strength and ductility are comparable to alloy 7075 (19) which is the alloy targeted for replacement by the test material.

Being a dispersion hardened powder metal product, it was expected to provide good corrosion resistance properties (17,20). Round tensile specimens were removed from the test piece with the loading oriented through the thickness. Specimens were subjected to a constant load and exposed to an alternate emersion of 3.5 percent by weight sodium chloride solution in accord with ASTM G44 (21). The data are presented in Table 2. Results were interpreted in compliance with ASTM G64 (22), producing a rating of intermediate, "C," resistance to stress corrosion cracking, which was less than expected.

TABLE 2
PM ALUMINUM AL-905XL FORGING STRESS CORROSION TEST RESULTS

<u>Stress (ksi)</u>	<u>Yield Strength (%)</u>	<u>Test Time (hours)</u>	<u>Failure? Yes/No</u>	<u>Residual Strength (ksi)</u>
45	75	24	Yes	N/A
45	75	99	Yes	N/A
45	75	384.5	Yes	N/A
30	50	64	Yes	N/A
30	50	843	No	61
30	50	507	No	61
30	50	757	Yes	N/A
30	50	787	No	61
15	25	507	No	61

SECTION 4 PROCEDURES

Constant amplitude fatigue crack growth rate tests were conducted in compliance with ASTM E647 (23). A compact-type specimen with a width, W, equal to two inches and a thickness, B, of a quarter inch was used for both the constant load amplitude and the OL fatigue tests. All specimens had a (L-T) orientation. One of the first alloy AL-905XL OL tests used a load-ratio of 0.1. The crack opening load was less than the minimum dynamic load, consequently the velocity recovered prematurely as the opening load dropped below the minimum dynamic load. For all remaining tests, a load-ratio equal to 0.05 and a frequency of 15 Hz were used for both types of dynamic testing. A computer was used for automated test control and to log the data. As with the preliminary work on alloy 2091, a Fractomat Krack Gage® was used for the crack length measurement.

Data were generated in laboratory air for the two extremes in relative humidity, i.e., below 10 percent and in excess of 90 percent. For the low humidity air environment, the specimen was enclosed in a sealed plexiglass box. The bottom of the chamber had an inch layer of dried desiccant. The sealed chamber was allowed to stand for approximately two hours prior to commencing load cycling.

The high humidity tests used the same environmental chamber but rather than using the desiccant a capped bottle half filled with distilled water was heated along with laboratory air being bubbled through the water. An output tube passed through the bottle cap and was plumbed into the test chamber. A humidity meter was left inside the chamber to insure the humidity stayed above 90 percent.

As with the constant load amplitude tests, the overload tests control and data acquisition were computer automated. The test procedure consisted of shedding the dynamic loads, after 10 mils of crack extension to a final stress intensity range of $6 \text{ KSI}\sqrt{\text{in.}}$ in compliance with ASTM E647 (18). Data were recorded for every 5 mils extension or 50,000 load cycles whichever occurred first. A single 150-percent overload beyond the maximum constant amplitude load was applied and followed by resumption of the pre overload dynamic loading conditions. A 150-percent overload was used for the aluminum AL-905XL material because an 80- or 100-percent spike produced no change in crack opening load and only a slight reduction in velocity over

10 to 15 mils of post-overload extension. For the initial 10 mils of post-overload crack extension data was recorded with greater regularity. Generally, the test was allowed to continue till the post-overload fatigue crack velocity exceeded that existing immediately prior to the overload cycle and the crack opening load dropped below the pre-overload value.

The crack opening load was determined by interrupting the dynamic loading and slowing the load cycling to approximately 0.03 Hz. The load was ramped to 95 percent of the maximum dynamic load for five successive load cycles. Load and strain data were recorded on the unloading portion of the load cycle. A straight line was fitted to the load versus BFS data for the data segment where the load exceeded 65 percent of the maximum dynamic load. Crack opening load was taken to be where the load versus strain data plotted outside the scatter band of the data used in fitting the straight line. Of the five measurements, the high and low values were rejected and Pop_1 was taken to be the average of the remaining three. Results are summarized in Table 3.

TABLE 3
ALUMINUM ALLOY AL-905XL FORGING 150-PERCENT OVERLOAD
FATIGUE TEST RESULTS

15 Hz R = 0.05 Lab Air

A/W	R.H (%)	Pop/Pmax	da/dn @ OL (μ in./cyc.)	Delay Cycles (*10 ⁻³)
0.586	< 10	0.094	1.406	33
0.449	< 10	0.148	0.845	37
			Avg.	35
0.376	28	0.112	1.070*	55
0.450	28	0.125	0.902*	41
			Avg.	48
0.362	52	0.242	0.888	37
0.396	58	0.104	0.494	59
0.392	48	0.150	1.092	48
			Avg.	48
0.339	> 90	0.117	1.287	63.2
0.663	> 90	0.137	2.374	45.4
0.429	> 90	0.208	1.515	48.1
0.502	> 90	0.377	1.453	53.5
0.620	> 90	0.406	1.711	73.5
0.568	> 90	0.184	1.614	40.7
			Avg.	54.1

* R = 0.10

SECTION 5

RESULTS AND DISCUSSION

Constant load amplitude fatigue data are presented in Figure 5. Above a stress intensity range of 4 KSI \sqrt{in} , the effective stress intensity range, ΔK_{eff} was about 85 percent of the remote stress intensity range, ΔK . As ΔK decreases below 3 KSI \sqrt{in} , ΔK_{eff} also decreases to about 70 percent of that applied. At the same time the data sets separate. The high humidity air data shows additional retardation, in the near threshold region. Alloy AL-905XL showed much lower P_{op} than that measured for the alloy 2091-T851 plate material due to the finer grain structure, less crack deflection and increased homogenization of slip (24).

The OL test results were presented in Table 3. In Figure 5 for ΔK equal to 6.0 KSI \sqrt{in} , the corresponding velocity is just above where the two data sets separate. Following overload, the crack velocity dipped into the 10^{-7} inch/cycle range where the data sets are clearly separated. The high humidity and lab air environments produced increased delay for some of the tests and consideration test-to-test variation in the number of delay cycles, than found in the dry air environment. For the laboratory air average test results, the 28 percent relative humidity produced about the same delay as found in the 50 percent relative humidity environment. The saturated air test results show about the same amount of scatter as the laboratory air data but with a small increase in the number of delay cycles for some test as was expected after viewing the constant load amplitude fatigue crack growth data.

A plot of one of the normalized crack velocity, V_i/V_o , and crack opening loads, P_{op}/P_{op0} , are presented in Figure 6. Both the AL-905XL and Al 2091 blunted cracks recover more often than not in two stages: first the crack opening load dips below the recover line and the crack velocity increases significantly, this first stage is not always present. The second part has the velocity drop dramatically while the opening load crosses above the recovery line; this second stage was always present for overloads greater than 80 percent.

There is a dramatic contrast between the alloys AL-905XL and 2091 response to an overload. The test materials recovery extends over much greater amount of crack extension but required only a small fraction of the number of delay cycles. The drop in

Al 905 XL Forging

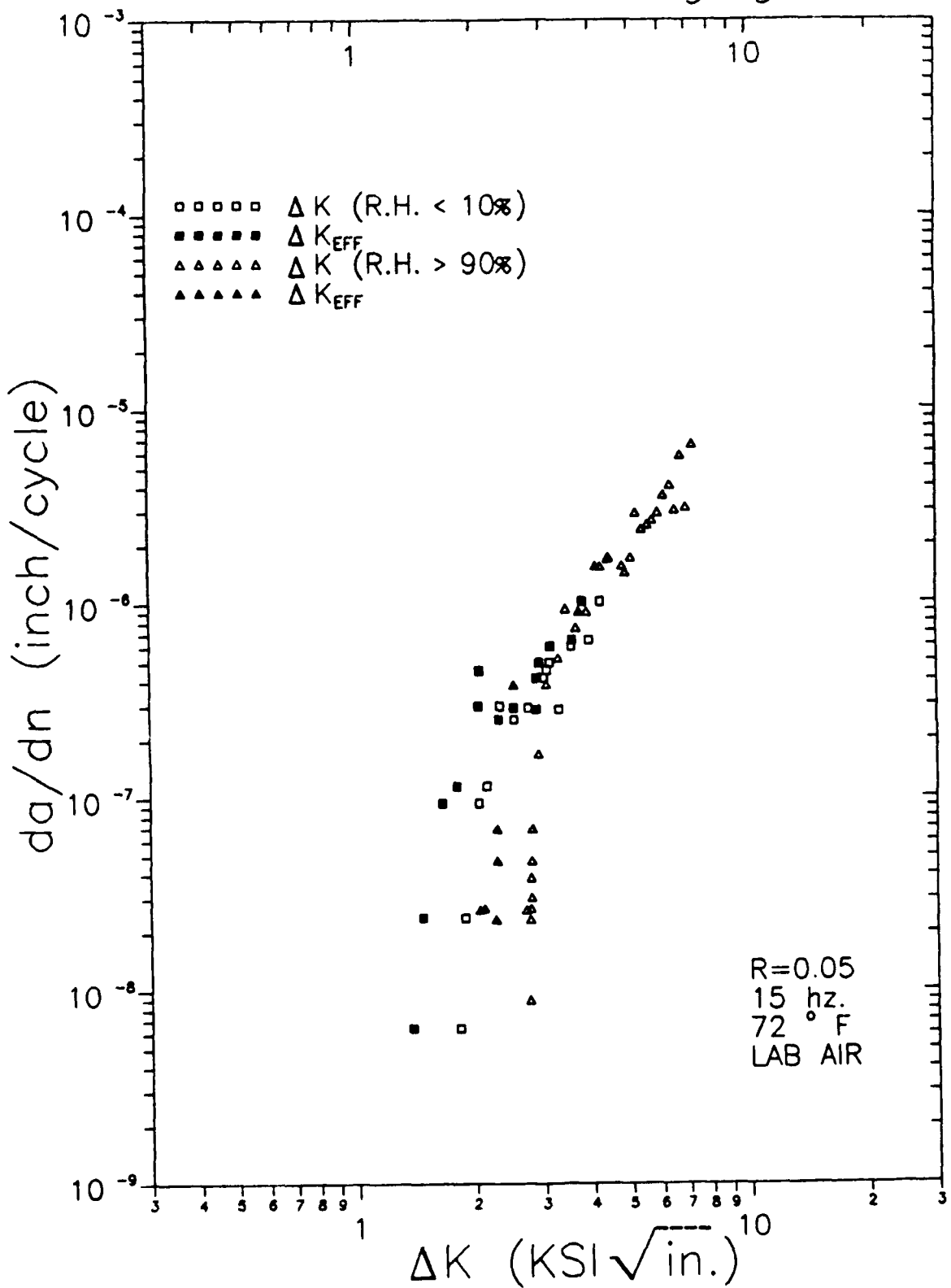


Figure 5. Constant Amplitude Loading High and Low Humidity Fatigue Crack Growth Test Results for Alloy AL-905XL Forging.

AI-Li POST-OVERLOAD RETARDATION

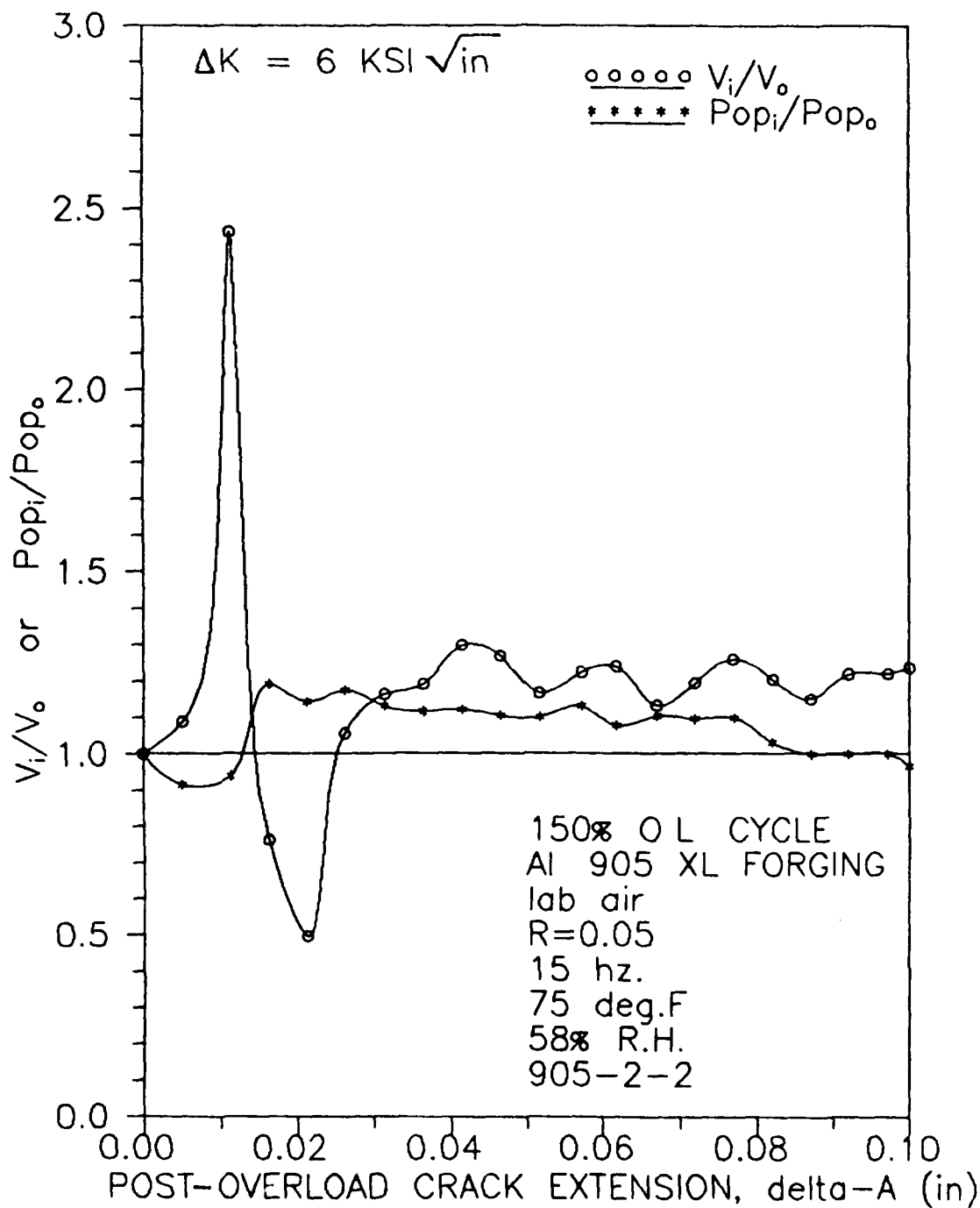


Figure 6. Post-Overload Normalized Velocity and Crack Opening Load Following a 150-Percent Overload on an Alloy AL-905XL Compact-Type Specimen.

crack velocity is much less than found in alloy 2091 even though the overload is nearly twice as much. The rise in post-overload crack opening load is much larger in the aluminum AL-905XL forging. In general, the precipitation hardened alloy 2091 showed much more retardation than the dispersion hardened test material.

In Figure 6, the crack velocity recovers following 0.025 inch of crack extension, whereas the crack opening load recovers following an additional 0.060 inch further extension. This occurred in both the high and low humidity environments, as well as, in the alloy 2091 tests and was believed to be due to the test procedure. In holding the post-overload dynamic loads constant, the crack is moving into an increasing stress intensity field. The stress intensity range increases from $6.00 \text{ KSI} \sqrt{\text{in.}}$ at the left side of the figure and to $6.69 \text{ KSI} \sqrt{\text{in.}}$ at tests end. Although nominally small, it is large enough to dominate the crack velocity and crack opening load. Increasing stress intensity produces more crack tip plastic zone residuals on which P_{op} is strongly dependent. The rising stress intensity bolsters P_{op} and postpones its dropping to the recovery line for thousands of additional load cycles. Simultaneously, the increasing K_{max} prematurely accelerates the crack velocity back to the recovery line; thus, the increasing stress intensity field drives the $P_{\text{op}}/P_{\text{op0}}$ and V_o/V_i traces final crossings of the recovery line in opposite directions.

Seeing this behavior in the test results, the procedure was altered to drop the dynamic loads after every 10 mils of post-overload crack extension, now keeping the stress intensity range ΔK at $6.0 \text{ KSI} \sqrt{\text{in.}}$ A few additional tests were conducted with the crack now moving into a constant stress intensity field. Results are summarized in Table 4. Plots for several of the tests are presented in Figures 7 through 9. As with the first series of tests, most recovered in two stages. Whether recovery is in one or two stages, now the two traces always cross the recovery line simultaneously or in close proximity. Recovery of the original velocity usually represented 0.040 to 0.060 inch of post-overload crack extension. In the dry and saturated air environments as the crack increases in length, the opening load and delay drop while the velocity increases. This was pursued further by taking the data from these tests where the stress intensity range was equal to $6.0 \text{ KSI} \sqrt{\text{in.}}$ either prior to OL or after recovery. The results are presented in Figures 10 and 11.

TABLE 4
ALUMINUM ALLOY AL-905XL FORGING 150-PERCENT OVERLOAD
FATIGUE TEST RESULTS

15 Hz R = 0.05 Lab Air $\Delta K = 6 \text{ KSI}\sqrt{in.}$

A/W	R.H (%)	Pop/Pmax	da/dn @ OL ($\mu \text{ in./cyc.}$)	Delay Cycles ($\times 10^{-3}$)
0.308	< 10	0.515	0.8544	42.9
0.374	< 10	0.457	1.2305	40.0
0.422	< 10	0.411	1.4105	37.9
0.555	48	0.116	1.1508	38.3
0.596	60	0.173	1.1415	127.1
0.631	58	0.143	1.0674	60.9
0.374	> 90	0.664	1.1283	89.9
0.494	> 90	0.326	2.0177	52.5
0.549	> 90	0.229	2.2777	41.9

* post-overload stress intensity range held constant at $\Delta K = 6 \text{ KSI}\sqrt{in.}$

AI-LI POST-OVERLOAD RETARDATION

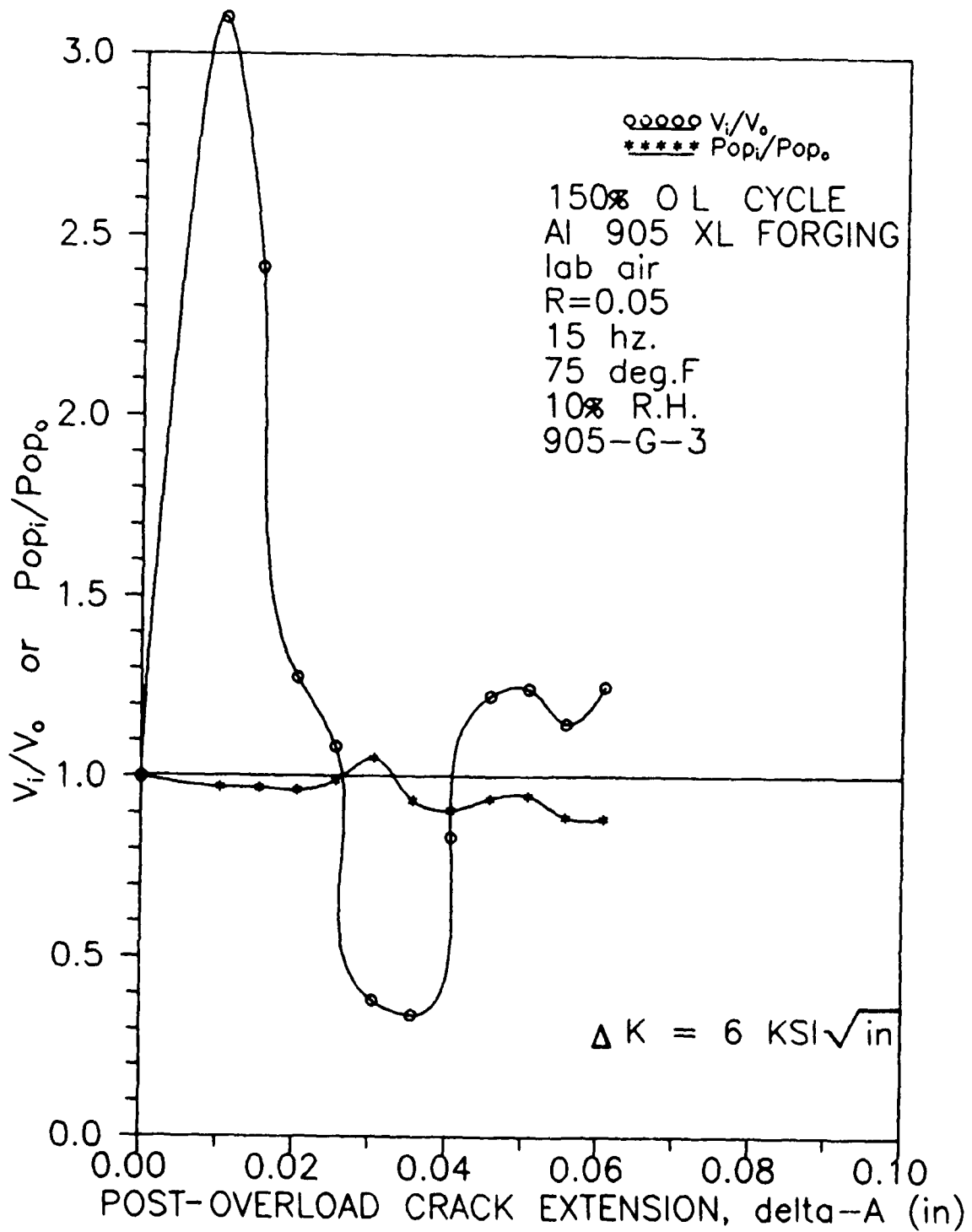


Figure 7. Post-Overload Normalized Velocity and Crack Opening Load Following a 150-Percent Overload on an Alloy AL-905XL Compact-Type Specimen in Low Humidity Air.

AI-Li POST-OVERLOAD RETARDATION

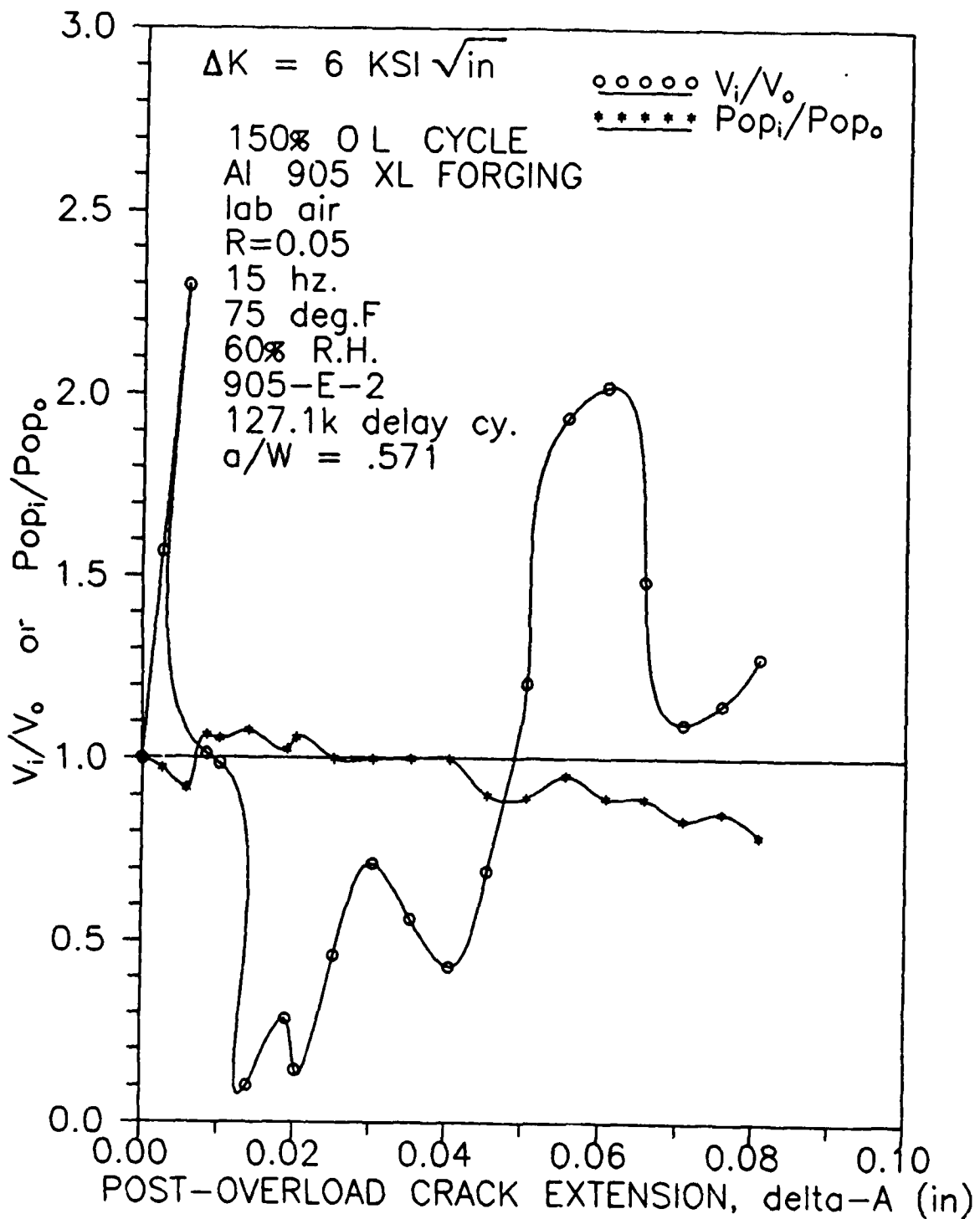


Figure 8. Post-Overload Normalized Velocity and Crack Opening Load Following a 150-Percent Overload on an Alloy AL-905XL Compact-Type Specimen in Laboratory Air.

AI-LI POST-OVERLOAD RETARDATION

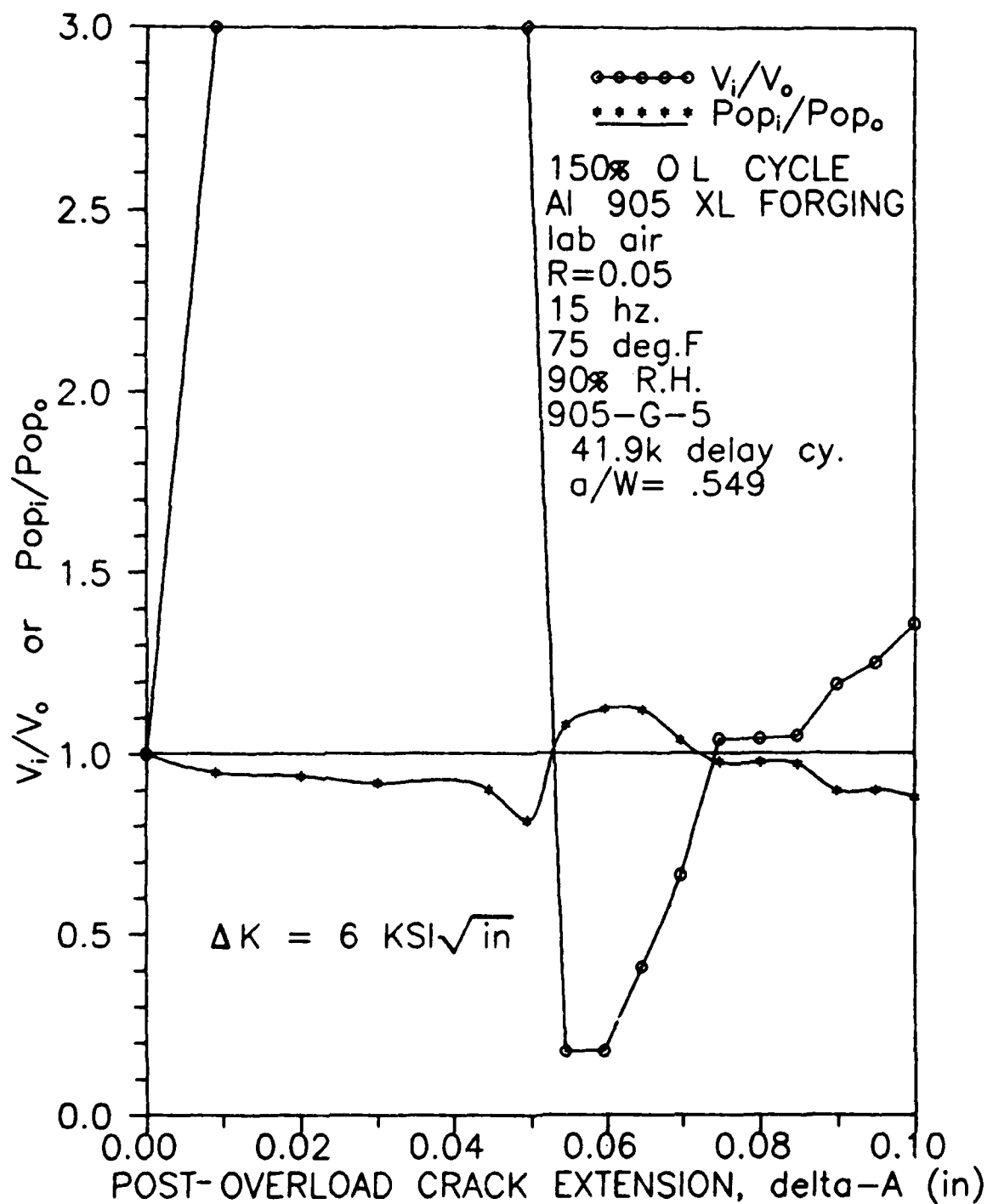


Figure 9. Post-Overload Normalized Velocity and Crack Opening Load Following a 150-Percent Overload on an Alloy AL-905XL Compact-Type Specimen in High Humidity Air.

Al 905 XL FORGING

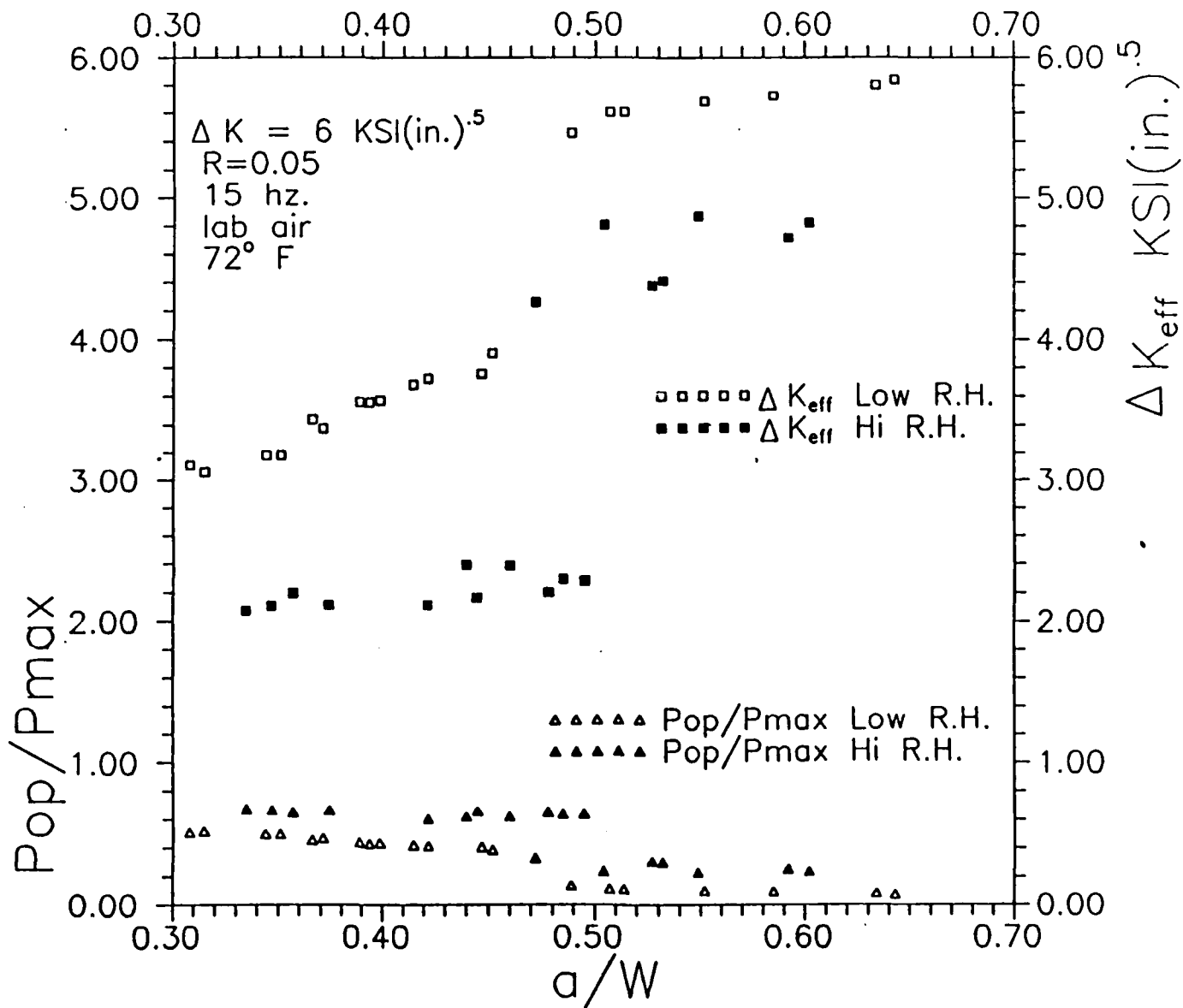


Figure 10. Alloy AL-905XL Normalized Crack Opening Load and Effective Stress Intensity Range for a Remote Stress Intensity Range Equal to $6 KSI\sqrt{\text{in.}}$

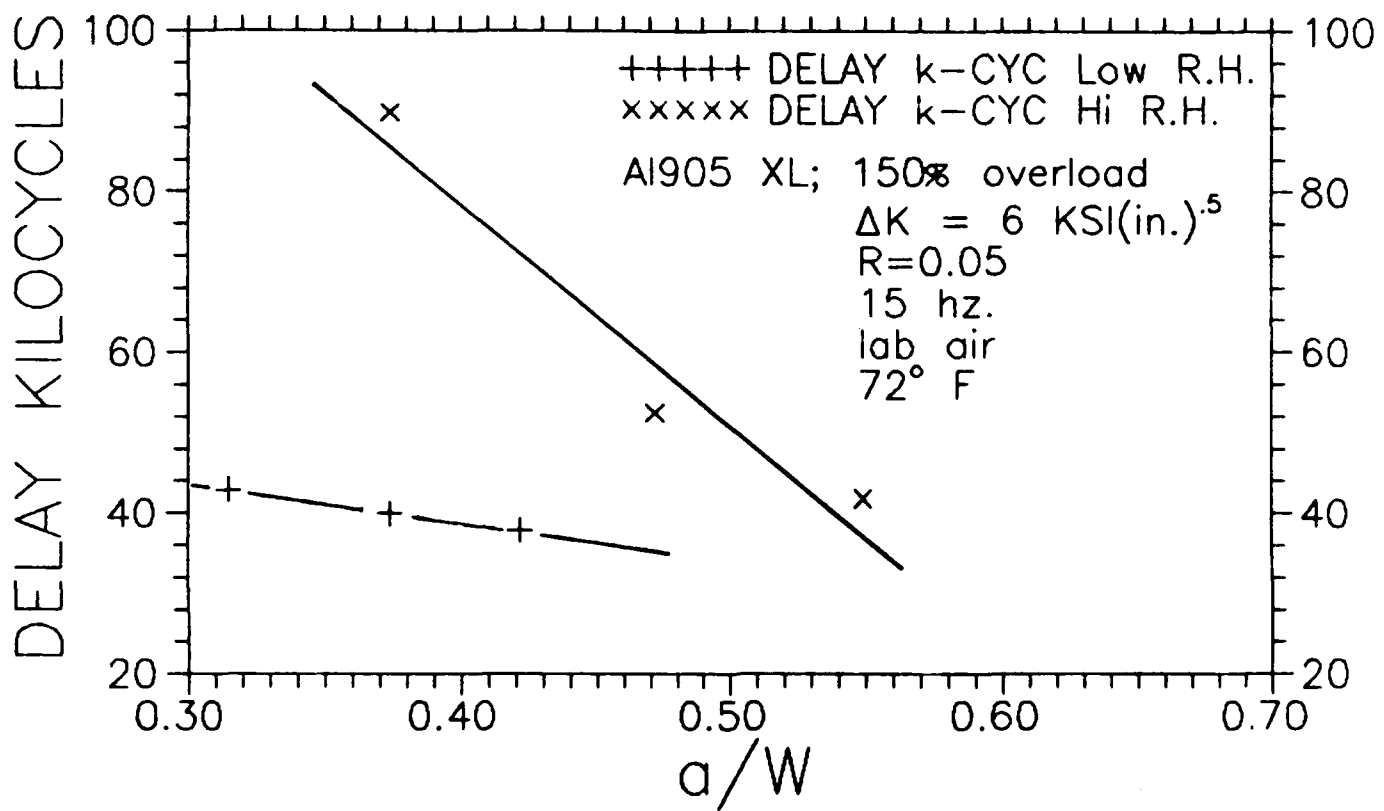


Figure 11. Post-Overload Delay Cycles for Alloy AL-905XL
 Following a 150-Percent Overload.

In Figure 10 the crack opening load is normalized with the peak dynamic load, P_{max} . The opening load drifts downward with crack extension. The dry air environments opening load is always lower than that for the saturated air. In the Figure ΔK_{eff} is smaller in saturated air. With increasing crack length ΔK_{eff} rises. The difference between the two data sets diminishes as the crack becomes longer and ΔK_{eff} approaches the remote stress intensity range, 6 KSI \sqrt{in} .

The delay cycles for the saturated and dry air tests are presented in Figure 11. At the left side of the figure, the delay is greater in the high humidity air due to oxidation products on the crack faces of a shorter tighter crack resulting in increased closure (4). If the dry air trend lines were extended, it would join that of the saturated air at an a/W value between 0.55 and 0.60 due to the crack remaining open for all of the load cycle, i.e. P_{op}/P_{max} equals the load-ratio of 0.05 (Figure 10).

SECTION 6

CONCLUSIONS

1. The retardation in crack growth rate due to compressive loads in spectrum loading seen in the dispersion hardened PM aluminum lithium test material, AL-905XL, was not near as great as that in alloy 2091 a precipitation hardened material.
2. In the constant load amplitude and overload experiments humidity produced an increase in fatigue crack growth resistance. For the OL tests increased retardation was reflected in a larger number of delay cycles.
3. The humidity-retardation effect diminishes with increased crack length where the crack tip remains open for more of the load cycle.
4. A small change in crack opening load can correspond to a great change in crack velocity.
5. It is more difficult to measure the crack opening load in an M(T) specimen than in a C(T) specimen particularly at shorter crack lengths.

REFERENCES

1. Bernard, P.J., Lindley, T.C., and Richards, C.E., "Mechanisms of Overload Retardation During Fatigue Crack Propagation," Fatigue Crack Growth Under Spectrum Loads, ASTM 595, American Society for Testing and Materials, 1976, pp. 78-97.
2. Elber, Wolf, "The Significance of Fatigue Crack Closure," Damage Tolerance in Aircraft Structures," ASTM STP 486, American Society for Testing Materials, 1971, pp. 230-242.
3. Peters, M., Welpmann, K., McDarmid, D. S., and Hart, W.G.J., "Fatigue Properties of Al-Li Alloys," AGARD Specialists' Meeting on New Light Alloys, Mierlo, Netherlands, October 1988, pg. 44.
4. McEvily, A.J., "On Closure Crack Growth," Mechanics of Fatigue Crack Closure, ASTM STP 982, J.C. Newman, Jr. and W. Elber, Eds., American Society for Testing and Materials, Philadelphia, 1988, pp. 35-43.
5. Venkateswara Rao, K.T., Bucci, R.J., Jata, K.V., and Ritchie, R.O., "A Comparison of Fatigue-Crack Propagation Behavior in Sheet and Plate Aluminum-Lithium Alloys," Materials Science and Engineering, Submitted August 1990.
6. Venkateswara Rao, K.T. and Ritchie, R.O., "Mechanics for Retardation on Fatigue Cracks Following Single Tensile Overloads: Behavior in Aluminum Lithium Alloys," Submitted to Acta Metallurgica, September 1987.
7. Buck, O., Federson, J.D., and Marcus, H.L., "Spike Overload and Humidity Effects on Fatigue Crack Delay in Al7075-T651," Fatigue Crack Growth Under Spectrum Loads, ATM 595, American Society for Testing and Materials, 1976, pp. 101-112.
8. Damage Tolerance Design Handbook, MCIC-HB-01R, December 1983, pp. 8.9-215.
9. Schelling, R.D., Gilman, P.S., and Donachi, S.J., "Aluminum-Magnesium-Lithium Forging Alloys Made by Mechanical Alloying," presentation at 17th National SAMPE Technical Conference, October 1985.
10. Petit, J., Suresh, S., Vasudevan, A.K., and Malcolm, R.C., "Constant Amplitude and Post-Overload Fatigue Crack Growth in Al-Li Alloys," Al-Li Alloys Vol. III, pp. 257-262.

11. Liaw, P.K., Logsdon, W.A., Roth, L.D., and Hartmann, H.R., "Krack-Gage for Automated Fatigue Crack Growth Rate Testing: A Review," Automated Test Methods for Fracture and Fatigue Crack Growth, ASTM STP 877, W.H. Cullen, R.W. Landgraf, L.R. Kaisand, and J.H. Underwood, Eds., American Society for Testing and Materials, Philadelphia, 1985, pp. 177-196.
12. MTS Extensometer and Clip Gage Catalog; 300022-05/632.00-05, MTS System Corporation, Minneapolis, Minnesota, 1986.
13. 1990 Annual Book of ASTM Standards, E399, Philadelphia, American Society for Testing and Materials, pp. 130-145.
14. Maxwell, D.C., "Strain Based Compliance Method for Determining Crack Length for a C(T) Specimen," AFWAL-TR-87-4046, July 1987.
15. Richards, C.E. and Deans, W.F., "The Measurement of Crack Length and Load Using Strain Gages," The Measurement of Crack Length and Shape During Fracture and Fatigue, C.J. Beevers, Ed., EMAS, Cradley Heath, UK, 1980, pp. 28-68.
16. Perkins, A.S., "Effect of Single Overload Upon Fatigue Crack Growth in an Aluminum-Lithium Alloy," AFIT/GAE/ENY/89D-27, December 1989.
17. Shrimpton, G.R.D. and Angus, H.C., "Aluminum Lithium Alloy Forging for Aerospace," SAE Technical Paper Series 881404, October 1988, pg. 2.
18. 1990 Annual Book ASTM Standard, E8-89G, Philadelphia, American Society for Testing and Materials.
19. Military Standardization Handbook, Metallic Materials and Elements for Aerospace Vehicle Structures, MIL-HDBK-5D, Vol. 1, 1 June 1983.
20. Benjamin, J.S. and Schelling, R.D., "Dispersion Strengthened Aluminum - 4 Pct Magnesium Alloy Made by Mechanical Alloying," The American Society for Metals and Metallurgical Society of AIME, Volume 12A, October 1988.
21. 1987 Annual Book of ASTM Standards, G44, Philadelphia, American Society for Testing and Materials, pp. 262-267.
22. 1987 Annual Book of ASTM Standards, G64, Philadelphia, American Society for Testing and Materials, pp. 352-356.
23. 1990 Annual Book of ASTM Standards, E647, Philadelphia, American Society for Testing and Materials, pp. 648-668.

24. Jata, K.V., Ruch, W., and Starke, E.A., "The Fatigue and Fracture Behavior of Al-Li-X Alloys Produced by Mechanical Alloying and Ingot Metallurgy Methods," MRS-Europe, November 1985, pp. 55-62.